The O I line emission in Active Galactic Nuclei revisited

A. Rodríguez-Ardila[1,2] and S. M. Viegas

Instituto Astronômico e Geofísico - Universidade de São Paulo, Av. Miguel Stefano 4200, CEP 04301-904, São Paulo, SP, Brazil

M. G. Pastoriza

Departamento de Astronomia - UFRGS. Av. Bento Gonçalves 9500, CEP 91501-970, Porto Alegre, RS, Brazil

L. Prato[1]

Department of Physics and Astronomy, UCLA, Los Angeles, CA 90095-1562

and

Carlos J. Donzelli

IATE, Observatorio Astronómico, Universidad Nacional de Córdoba, Laprida 854, 5000, Córdoba, Argentina.

ABSTRACT

UV, visible, and near−infrared spectroscopy is used to study the transitions of neutral oxygen leading to the emission of broad O I $\lambda8446$, $\lambda11287$ and $\lambda1304$ in Active Galactic Nuclei. From the strength of the former two lines, contrary to the general belief, we found that in six out of seven galaxies, Lβ fluorescence is not the only mechanism responsible for the formation of these three lines. Because O I $\lambda13165$ is almost reduced to noise level, continuum fluorescence is ruled out as an additional excitation mechanism, but the presence of O I $\lambda7774$ in one of the objects suggests that collisional ionization may have an important role in the formation of O I $\lambda8446$. The usefulness of the O I lines as a reliable reddening indicator for the broad line region is discussed. The values of E(B-V) derived from the $\lambda1304/\lambda8446$ ratio agree with those obtained using other reddening indicators. The observations point toward a break in the one-to-one photon relation between $\lambda8446$ and $\lambda1304$, attributable to several destruction mechanisms that may affect the latter line.

---

[1]Visiting Astronomer at the Infrared Telescope facility, which is operated by the University of Hawaii under contract from the National Aeronautics and Space Administration

[2]e-mail address: ardila@iagusp.usp.br

Subject headings: galaxies: Seyfert – radiation mechanisms — galaxies: nuclei

1.   Introduction

Permitted transitions of O I in the spectra of gaseous nebulae are very important tracers of atomic processes other than recombination, as well as indicators of the physical conditions of the emitting gas. For many years, O I $\lambda 8446$, usually the strongest O I line in the optical region, has been broadly studied in a large number of objects such as the Orion nebula (Morgan 1971; Grandi 1975), planetary nebulae (Grandi 1976), and the pre−main-sequence Herbig AeBe star LkHα 101 (Rudy et al. 1991). In active galactic nuclei (AGN), this feature is very common. Grandi (1980) presented observational data showing that its strength could reach several percent of Hα. He associated the O I emission with a phenomenon restricted to the broad line region (BLR). Later, Morris & Ward (1989) showed the lack of detectable O I $\lambda 8446$ in Seyfert 2 galaxies, confirming earlier predictions.

Usually, resonance fluorescence by Lyβ has been invoked as the single dominant mechanism for the production of O I $\lambda 8446$ in AGN since Grandi (1980). This process is favored by a coincidence of energy levels between O I and H I: the $2p\ ^3P - 3d\ ^3D^0$ transition of O I at 1025.77 Å falls within the Doppler core of Lyβ (1025.72 Å) for gas at 10^4 K, a temperature that is easily reached in the BLR. If this process is the dominant one, O I $\lambda 11287$ and O I $\lambda 1304$ should also be observed, since they are by-products formed during the cascading to the ground level following the absorption of a Lyβ photon. In addition, the photon flux ratio between $\lambda 11287$ and $\lambda 8446$ should be unity since every $\lambda 11287$ photon leads to the emission of exactly one $\lambda 8446$ photon. Smaller values of this ratio should indicate the presence of recombination, continuum fluorescence, or other processes that enhance $\lambda 8446$ but not $\lambda 11287$.

Determining the mechanisms leading to the O I emission in AGN is important for various reasons. If Lyβ fluorescence is dominant, photons of this line are converted to those of neutral oxygen, affecting the population of the excited levels of hydrogen. This process would act as a cooling agent for the regions where the hydrogen lines are very optically thick. Therefore, it is a process that must be taken into account when using photoionization modeling to describe the state of the BLR. Also, the O I lines can be used as a reliable reddening indicator for the BLR if the contributions of the different processes to the line flux are known in advance.

To the best of our knowledge, the only simultaneous detection of O I $\lambda 8446$ and $\lambda 11287$ in an AGN was reported by Rudy et al. (2000) for I Zw 1. Previously, Rudy, Rossano & Puetter (1989) reported the detection of O I $\lambda 11287$ for that same object. Combining previous measurements of $\lambda 8446$ taken from Persson & McGregor (1985), Rudy, Rossano & Puetter (1989) found that the ratio of photon fluxes between these two lines was equal to unity, providing a direct confirmation that the broad permitted O I lines observed in an AGN arise through Lyβ fluorescence. Interestingly, in the spectrum of I Zw 1 recently published by Rudy et al. (2000), with a higher resolution and spectral

coverage, the photon flux ratio between $\lambda11287$ and $\lambda8446$ that we derive from their data is 0.76. If this ratio is corrected for the E(B-V) of 0.16 adopted by these authors, it does not appreciably change, but decreases to 0.74. Thus, contrary to what has been claimed, Lyβ fluorescence seems not to be the only mechanism contributing to the production of $\lambda8446$.

We have started a program to simultaneously measure O I $\lambda8446$, $\lambda11287$ and $\lambda13165$ in a sample of AGN. Our goal is to establish if there is an excess of $\lambda8446$ emission, as in I Zw 1, indicating that Lyβ fluorescence is not the only excitation process that may give rise to the broad permitted O I lines. For this purpuse, near-infrared spectroscopy at moderate resolution (R$\sim$320 km/s) covering the spectral range 0.8μm – 2.4μm was obtained. By combining these observations with quasi-simultaneous visible spectroscopy and archival HST/IUE spectra, we expect to obtain additional information about the radiation processes that govern the O I emission and to test the usefulness of the O I lines as a reddening indicator for the BLR. The observations are presented in §2, a review of the principal mechanisms for the production of the O I lines is given in §3. A discussion of the results appears in §4. Our conclusions are in §5.

2. Observations

2.1. The sample

The sample of galaxies used in this work is composed of six narrow-line Seyfert 1 galaxies (NLS1s) and one classical Seyfert 1 galaxy. All seven objects show bright O I $\lambda8446$, so it is expected that if Lyβ is the dominant excitation mechanism for the O I emission, O I $\lambda11287$ should also be present at a similar intensity. In addition, data in the UV and optical region are available for the selected sample to help to distinguish other processes that can also contribute to the formation of broad O I lines. The reason for the predominance of NLS1s in the sample is that permitted lines in these objects are relatively narrow, minimizing the effects of blending with adjacent features. For example, the red wing of $\lambda8444$ is very close in wavelength to the two Ca II lines located at $\lambda8498$ and $\lambda8542$. Table 1 lists the objects selected for this study as well as their relevant characteristics. Except for I Zw 1, for which the flux measurements were drawn from the literature, our own observations or archival data are used for the remaining objects, as described in the following sections.

2.2. Near-infrared spectroscopy

Near-infrared spectra providing continuous coverage between 0.8 μm and 2.4 μm were obtained at the NASA 3 m Infrared Telescope Facility (IRTF) on 2000 October 11 (UT) with the SpeX facility spectrometer (Rayner et al. 2001). The detector consists of a 1024×1024 ALADDIN 3 InSb array with a spatial scale of 0.″12/pixel. Simultaneous wavelength coverage is carried out by means

of prism cross-dispersers. A $0.8'' \times 15''$ slit was used during the observations, giving a spectral resolution of 320 km/s. The seeing was near $1''$ during the exposures. Table 2 summarizes the log of these observations.

Details of the spectral extraction and wavelength calibration procedures are given in Rodríguez-Ardila et al. (2002). The spectral resolution was sufficiently high so that in all cases O I $\lambda 8446$ could be cleanly isolated from the Ca II lines. O I $\lambda 11287$ is located in a region free of nearby emission features, so its line profile is well defined. Figure 1 shows the observed O I lines plotted on a laboratory wavelength scale.

2.3. Optical Spectroscopy

Optical spectra covering simultaneously Hα and Hβ were available for all the target objects except NGC 863. Long-slit spectroscopic observations of 1H 1934-063, Mrk 335, Mrk 1044 and TON S 180 were obtained with the Complejo Astronómico El Leoncito 2.15 m telescope using a TEK 1024×1024 CCD detector and a REOSC spectrograph. A 300 line mm^{-1} grating with blaze angle near 5500 Å and a spatial scale of $0.''95$ pixel^{-1} was used, giving an instrumental resolution ~ 8 Å. The slit, with a width of $2.''5$, was oriented in the east-west direction. Spectra were reduced with stardard IRAF procedures (i.e. bias subtraction and flat field division). The signal along the central 4 pixels was summed to extract the spectra. Wavelength calibration was carried out using HeNeAr arc lamps, with typical errors of less than 0.1Å. Standard stars from Stone & Baldwin (1983) were used for flux calibration. In addition, a medium-resolution spectrum (~ 3 Å) of 1H 1934-063, taken with that same telescope and covering the wavelength interval $6050 - 7600$ Å, was also available. In the remainder of this text, we will refer to the spectrum of 1H 1934-063 taken with the 300 line mm^{-1} grating as the low-resolution spectrum and the one taken with the 600 mm^{-1} grating as the high-resolution spectrum.

Ark 564 was observed in 1996 with the *HST* using the Faint Object Spectrograph (FOS) with a circular aperture $1''$ in diameter. For this object, we retrieved the calibrated files from the *HST* data archive to obtain the wavelength, absolute flux and error flags. A log of the optical observations is listed in Table 2.

2.4. Ultraviolet Spectroscopy

Ultraviolet spectra observed by the *IUE* and the *HST* (FOS and STIS), in the wavelegth region around O I $\lambda 1304$ are available for all objects of the sample. The *IUE* spectra were re-extracted using the IUE New Spectral Image Processing System (NEWSIPS). When more than one observation for a given object was available, they were combined in order to produce a single, averaged spectrum. FOS and/or STIS nonproprietary archival calibrated files for Ark 564, Mrk 335 and TON S 180 were retrieved from the *HST* data archive. Ark 564 has been the subject of a monitoring campaing using

STIS during the year 2000, so we averaged calibrated archival files taken between May and July 2000. We compared the resulting spectrum with the FOS spectrum taken for this same object in 1996 and no significant difference was found in the region around $\lambda1304$. However, we preferred to work with the STIS spectrum because of the better resolution and S/N, which allowed us to separate, at a higher confidence level, the flux of O I $\lambda1304$ from that of Si II $\lambda1306$. Table 3 shows the details of all UV observations used in this work.

Figure 2 show the composite near-IR, optical and UV spectra for the galaxy sample. The arrows mark the position of the strongest O I lines that are of interest here.

2.5. Further considerations

Before any analysis, the spectra were corrected for Galactic reddening using the values reported in Table 1. Although different apertures were used during the observations, this has little effect on the results reported here, since our analysis is restricted to lines emitted exclusively by the BLR. Table 4 lists the galaxy sample emission line fluxes that will be used throughout this paper. The erros quoted reflect solely the uncertainty in the placement of the continuum, S/N around the line of interest and erros flags of the archival data and are 2σ significative. Fluxes were measured by fitting Gaussians to each emission feature. In all cases, O I $\lambda11287$ and O I $\lambda8446$ were well described by a single Gaussian of similar width. In the optical region, if [N II] $\lambda\lambda6548$ and 6583 were present, their contribution was always subtracted before deriving the flux for Hα. The strong Fe II emission that contaminates the wings of Hβ and He II $\lambda4686$ was subracted before measuring the flux of these two lines. For this step, the method used was that described by Boroson & Green (1992), consisting of modeling the Fe II lines using a Fe II template from I Zw1.

The greatest uncertainty comes from the measurement of O I $\lambda1304$, mainly in *IUE* data. This line (actually a triplet at $\lambda1302.17$, $\lambda1304.86$, and $\lambda1306.0$) is severely blended with Si II $\lambda\lambda1304,1309$. In order to separate the O I contribution, we used the prescription described in Laor et al. (1997). This consists of assuming a Si II $\lambda1309/\lambda1304$ ratio of either 2 (optically thin case) or 1 (optically thick case). This method can be applied only if Si II $\lambda1309$ is clearly detected, as is the case for Ark 564, Mrk 335 and TON S 180. As in Laor et al. (1997), we assumed an optically thick Si II doublet given that for all objects of our sample the Mg II ratio $\lambda2796/2804$ falls between 2 and 1. In 1H 1934-063, Mrk 1044 and NGC 863, the deblending procedure is more uncertain because of the much lower *IUE* spectral resolution. For these objects, we assumed that 75% of the flux in the $\lambda1304$ feature was due to O I. That was the average proportion found in the three objects where the deblending was possible.

2.5.1. Variability

Another source of error that may affect our results when combining data from different spectral regions, taken at different dates, is variability. It is widely known that Seyfert 1 galaxies are highly variable in the UV and optical continuum and broad emission lines. However, there is little information in the literature about optical and/or UV variability in NLS1s, even though they show the fastest variations in the soft and hard X-ray bands. Giannuzzo & Stirpe (1996) systematically monitored a sample of 12 NLS1 during a period of one year and found that 10 of them showed significant variations in the optical continuum and permitted lines. Ark 564 and Mrk 1044, two of the objects from our sample included in Giannuzzo & Stirpe's study, showed variations of $\sim$9% and $\sim$10%, respectively, in permitted lines Hα and Hβ. More recent data for Ark 564 derived from a two-year optical monitoring program (Shemmer et al. 2001) showed that Hβ exhibited only minor variability ($\sim$3%) and that Hα did not vary significantly. In the UV region, Collier et al. (2001), using STIS data taken from an intensive two-month monitoring campaing, found flux variations of about 1% amplitude in the Lyα emission line. Moreover, they checked archival *IUE* observations of Ark 564 taken in Jan 1984 and compared these data with that of STIS. They found that the continuum and emission line fluxes are in qualitative agreement in spite of the long span of the observations.

For TON S 180, we have compared archival *IUE* spectra taken in 1992 and 1993 with that of STIS used in the present work. Although the continuum from IUE presents a shift towards larger flux values (in a constant amount) relative to the STIS spectrum, the line fluxes shows very little difference (by less than a factor of 10%) between the two set of observations. In addition, our flux measurement for Hβ taken in 2000 is in perfect agreement with that reported by Winkler (1992), ruling out significant variations for that object.

Mrk 335 was monitored continuously in the optical region during a seven year campaing (Kassebaum 1997). This NLS1 shows significant variability in the continuum as well as in the emission lines Hβ and He II λ4686 with RMS fluctuation amplitude relative to the mean spectrum of 8.5%, 7% and 18.8%, respectively. No UV variability data for this object have been reported. For 1H 1934-063 and NGC 863 no information about variability in the optical/UV region is available in the literature. Optical follow-up taken for other NLS1s not included in this work, such as NGC 4051 (Peterson et al. 2000) during a three-year campaing, shows RMS fluctuation amplitude relative to the mean spectrum of 9.5% in Hβ.

From above, it can be seen that variability has little effect on our data. Even adopting a conservative error of 10% when combining UV/near-IR or UV/optical measurements, that estimate is within the uncertainties due to the deblending and S/N of the UV lines. Moreover, due to the fact that the O I lines are formed in the outermost portion of the BLR (see Rodríguez-Ardila et al. (2002)), it is expected that their variability amplitude be even smaller that that found for other broad line features.

3. Excitation mechanisms of the O I lines

O I $\lambda 8446$ can be produced by four known mechanisms: recombination, collisional excitation, continuum fluorescence, and Lyβ fluorescence. Grandi (1980), Rudy, Rossano & Puetter (1989), and Rudy et al. (1991) gave a complete review of these four processes. For this reason, here we will only focus on the resulting O I emission lines arising from each of them.

Besides O I $\lambda 8446$, recombination and collisional excitation also forms O I $\lambda 7774$, while continuum fluorescence forms O I $\lambda 7002$, $\lambda 7524$ and $\lambda 13165$. Lyβ fluorescence, also known as Bowen Fluorescence, does not produce neither of the last four lines; their absence is a good indicator of the predominance of this mechanism. Lyβ fluorescence takes advantage of the near coincidence of the energy levels of Lyβ (1025.72 Å) and the $2p\ ^3P - 3d\ ^3D^0$ transition of O I at 1025.77, as can be seen in Figure 3. At 10^4 K, a typical temperature within the BLR, the difference in wavelength falls within the Doppler core of Lyβ. When excitation to the $3d^3D^0$ occurs, the O I electron may return directly to the ground state or otherwise suffer a series of transitions producing photons at $\lambda 11287$, $\lambda 8446$, and $\lambda 1304$ before arriving at the ground state.

Until now, Lyβ fluorescence has been the favoured mechanism for the production of $\lambda 8446$ in AGN (Oke & Shields 1976; Grandi 1980; Morris & Ward 1989; Rudy, Rossano & Puetter 1989). The reason for this conclusion has been the apparent lack of detection of additional O I transitions such as $\lambda 7002$ and $\lambda 7774$. However, weak broad features in low resolution spectra tend to be smeared out when the nuclear continuum is strong and the S/N low. A direct confirmation of the predominance of the Bowen fluorescence can be obtained by measuring the photon flux ratio between $\lambda 11287$ and $\lambda 8446$, which must be unity (assuming no internal reddening). Lower values would indicate the presence of one of the other three mechanisms mentioned above, or some combination of these. This test has been elusive in AGNs for many years because of the lack of suitable observations and dectectors in the near-IR. To the best of our knowledge, the only detection of O I $\lambda 11287$ to date in an AGN has been for the prototype NLS1 I Zw 1.

Nonetheless, we find an inconsistency in the published data. Rudy, Rossano & Puetter (1989) provided a direct confirmation of the Bowen mechanism in I Zw 1 by deriving an O I $\lambda 11287/\lambda 8446$ photon flux ratio of 1.02. Using more recent and higher quality data, taken at a higher resolution by Rudy et al. (2000) for the same object, we derive a photon flux ratio of 0.76 using the emission line flux reported by those authors in their Table 1. Rudy, Rossano & Puetter (1989) combine data taken at different times with a different instrumental setup and resolution, while in Rudy et al. (2000), both lines are observed simultaneously, with a superior quality spectrograph. Our estimate implies that in I Zw1, contrary to what was previously found, O I $\lambda 8446$ is formed by more than one process.

Table 5 lists, in column 2, the O I $\lambda 11287/\lambda 8446$ (hereafter $\mathrm{ROI_{IR}}$) flux ratio and, in column 3, the photon flux ratio of these two lines, derived for the objects in our sample. Only in TON S 180 and Ark 564, does the observational evidence points to Lyβ fluorescence as the dominant mechanism for the production of $\lambda 8446$ since the photon flux ratio is near unity. But in Mrk 1044, for example,

Lyβ fluorescence accounts for only $\sim$40% of the observed λ8446. Evidently, additional excitation mechanisms that enhance O I λ8446 relative to λ11287 are at work. Reddening cannot be invoked to explain this discrepancy because its net effect is the opposite: to reduce O I λ8446 relative to λ11287. If the line ratios in Table 5 are affected by reddening, after correcting for this effect they will appear even smaller.

It may be argued that the deficit of λ11287 photons can be due to strong, sharp, atmospheric absortion lines not readily apparent in low-resolution spectra. If such a line falls near λ11287 (in the Earth-frame wavelength), it can substantially affect the measured flux of the latter. Kingdon & Ferland (1991) addressed this possibility in his study of He I λ10830 in planetary nebulae and concluded that this effect could reduce the intensity of He I λ10830 by as much as 20%$-$25%. Nonetheless, as he stressed, the effect can be dramatic in sharp-lined objects such as HII regions and planetary nebulae. For the particular case of O I λ11287, this line is spread over at least 21 pixels (the narrowest full width at zero-intensity measured for O I λ11287) and located in different regions of the CCD due to the different redshifts of the objects.

We consider that for O I λ11287, the most serious effect is not due due to strong, sharp, atmospheric absortion lines but broad atmospheric bands located blueward of λ11287. If they are not adequately cancelled out after dividing the object's spectrum by that of the telluric star, the shape and flux of the line can be seriously affected. Figure 4 shows, for every object, the observed spectrum, the spectrum of the telluric star observed at similar airmass, and the resulting spectrum after the division, in the region around O I λ11287. Note that in all cases the atmospheric features were cleanly removed. Although some residuals may be present, by no way they do not affect the flux of λ11287. Also, the fact that the shape and width of λ11287 is essentially the same as that of λ8446 (see Rodríguez-Ardila et al. (2002)), confirms that the deficit of photons in O I λ11287 cannot be due to this effect. Regarding λ8446, the position where it falls is far from any atmospheric absorption feature. The nearest one is located redward of 9000 Å (in the Earth-frame wavelength) while for the galaxy with the largest redshift (TONS180), O I λ8446 is located at 8970 Å.

4.   Discussion

The results obtained in the last section provide, for the first time, strong evidence that Lyβ fluorescence cannot be the only process responsible for the observed strength of O I λ8446 in most AGNs of our sample. In order to study which of the remaining three mechanisms already mentioned (continnum fluorescence, recombination and collisional ionization) are also producing λ8446, we use other permitted lines of O I as diagnostics tools.

According to Grandi (1980), continuum fluorescence can be probed by the presence of O I lines such us λ7254, λ7002 and λ13165. The later line is, in fact, a very good test because it should be one of the strongest ones, with a strength similar to that of λ11287, if that process is present. Unfortunately, observing λ13165 is not always easy. Depending on the radial velocity of the galaxy,

it may fall very near or within a strong atmospheric band located between 13300 Å and 14150 Å, preventing its observation.

We have searched carefully in the spectra for the presence of O I $\lambda13165$. No conclusive evidence of this line was found in any galaxy. Upper limits derived for its flux are listed in Table 4. In all cases, it is detected at a limit of $<0.1F_{\lambda11287}$. In TON S 180 and NGC 863 it is not observable at all because it falls within a region of poor transmission. We also searched for O I $\lambda7002$ and $\lambda7254$ in 1H 1934-063. In the high resolution spectrum of this object, the former line is clearly present, as can be seen in Figure 5. For the latter line, an upper limit for its flux was derived. Table 6 lists the values found. For Ark 564, no trace of $\lambda7002$ can be seen in the spectrum published by Comastri et al. (2001).

The lack of additional O I lines that should be observed if continuum fluorescence is also responsible for $\lambda8446$ emission and, most importantly, the very low upper limit measured to O I $\lambda13165$, leads us to conclude that this mechanism, although probably present, cannot be responsible for the observed excess of O I $\lambda8446$ emission.

Recombination is another excitation mechanism that could help to explain the strength of O I $\lambda8446$. However, this process produces numerous lines located in the visible region, arising from triplet and quintet configurations, in proportions corresponding to the ratio of their statistical weights (Grandi 1975). This implies that some of the additional O I lines should have comparable or larger intensities than O I $\lambda8446$. In 1H 1934-063, for which we have complete wavelength coverage from 0.37μm to 2.4μm, the only quintet line of O I detected at 3σ level is $\lambda7774$ ($3s^5S - 3p^5P$). This line is the quintet counterpart of O I $\lambda8446$. Its predicted relative intensity, assuming recombination as the excitation mechanism, should be $\lambda7774/\lambda8446 \sim1.7$ (Grandi 1980). That value is 40 times higher than the observed one ($\lambda7774/\lambda8446 \sim0.07$, see Table 6). For this object, if we subtract the fraction of the O I $\lambda8446$ flux produced by Lyβ fluorescence, the resulting $\lambda7774/\lambda8446$ ratio is 0.2, nearly 20 times weaker than its theoretical prediction.

The other object for which observations around O I $\lambda7774$ are available is TON S 180. The upper limit derived for this feature, also listed in Table 6, is two orders of magnitude weaker than the theoretical prediction. However, it is not expected that this line be strong in TON S 180 since Lyβ fluorescence accounts for the total O I $\lambda8446$ emission.

In addition to O I $\lambda7774$, we detect in 1H 1934-063, O I $\lambda7990$ (see Figure 5) and $\lambda6048$. A blip at this later position is also observed in the spectrum of Ark 564. Nonetheless, their intensities are always a few percent of O I $\lambda8446$. For this reason, we conclude that recombination is certainly present but it cannot explain alone the excess of $\lambda8446$ observed in most of the objects.

The only possibility that remains to be explored is collisional excitation by electrons. Grandi (1980) states that if this mechanism is operating, the predicted O I $\lambda7774/\lambda8446$ ratio would be 0.3. That value is near the observed ratio (0.2) derived in 1H 1934-063 after removing the contribution of Lyβ fluorescence for O I $\lambda8446$. The lack of observations around $\lambda7774$ for the remaining objects prevent us from drawing definite conclusions. However, our data clearly show that Lβ

fluorescence cannot be considered any longer as the single dominant mechanism for the production of the observed O I lines in AGN. For 1H 1934-063, for instance, collisions may contribute up to 35% of the observed O I λ8446 flux.

4.1. An optically thick λ1304 line?

If collisional excitation is responsible for the excess of O I λ8446 emission, in order to this process be efficient the population of the level $3s^3S^0$ must be significant, i.e. above the Boltzman population. This requires high optical depths in the λ1304 line. Kwan & Krolik (1981) state that with increasing column density, trapping of λ1304 becomes important in sustaining the population in $3s^3S^0$, and λ8446 becomes optically thick. Trapping of λ8446, in turn, builds up the population in $3p^3P$, eventually leading to trapping of λ11287. As a result, the growth of these lines is subsequently quenched; once λ11287 is optically thick, all three lines grow only logarithmically with optical depth. This possibility has been examined by Ferland & Persson (1989), who found that the very high column densities ($>10^{24.5}$ cm^{-2}) necessary to produce Ca II can produce large optical depths in the O I lines. In fact, very recently, Rodríguez-Ardila et al. (2002) found that the O I, Ca II and Fe II lines have very similiar emission line profiles, both in form and width. This is interpreted as a co-spatial Ca II and O I emitting regions, which probably share similar physical conditions.

An indication that λ8446 is thick would be branching from its upper level to 3^5S, by the O I] λ6726 line (Rudy et al. 1991). This line is very close to [S II] λ6717,6731, a commom doublet in Seyfert 1 galaxies, so if this pair of lines is present, it may mask the observation of O I] λ6726. We have searched our spectra in order to find evidences for λ6726. Table 6 list the derived upper limits. In none of the four objects where this measurement was possible was the λ6726 line present at a level greater than $0.04I(\lambda8446)$. We conclude that the intensity of λ8446 is not significantly altered by optical depth effects. Probably, after the upper $3p^3P$ level is significantly populated, the electrons are rapidly promoted to the upper $^3S^0$ and $^3D^0$ levels because of their close proximity in energy (less than 2 eV), producing the additional O I lines detected and increasing the flux of λ8446.

4.2. O I as a reliable reddening indicator for the BLR

According to the Grotrian diagram of Figure 3, independent of the excitation mechanism, every λ8446 photon should produce a λ1304 photon. Theoretically, the photon flux ratio λ1304/λ8446 (ROI$_{uv}$, hereafter) must be equal to unity except when reddening is present, in which case, it should be smaller. Kwan & Krolik (1981) found that the intrinsic ROI$_{uv}$ can vary from 1 to 0.63 even in the absence of reddening due to Balmer continuum absorption of λ1304 photons and the production of λ8446 by collisional excitation. Grandi (1983) describes three additional proccesses that may destruct λ1304: *(i)* λ1304 photons can photoionize H I atoms that exists in the $n = 2$ state; *(ii)*

collisional de-excitation can destroy $\lambda 1304$ photons; *(iii)* the upper term of $\lambda 1304$ ($3s\ ^3S^o$) can decay to the metastable terms of the ground configuration via the semi-forbidden lines O I] $\lambda 1641$ and $\lambda 2324$ ($2p^4\ ^1D$ - $3s\ ^3S^o$ and $2p^4\ ^1S$ - $3s\ ^3S^o$, respectively). Grandi's calculations show that up to half of the $\lambda 1304$ photons can be converted to O I] $\lambda 1641$ before leaving the emission cloud.

Our data offers, for the first time, the possibility of evaluating, at least to first order, how efficient the destruction of the $\lambda 1304$ photons can be. Column 5 of Table 5 lists the $\mathrm{ROI_{uv}}$ photon ratio derived for the galaxies. It was determined assuming an intrinsic flux ratio of 6.5. Note that the uncertainties in this quantity is, in most cases, larger that the estimated error due to variability (see § 2.5.1), meaning that the results are not at all affected by this effect. Except TON S 180, all objects show flux ratios significantly below the lowest theoretical limit derived by Kwan & Krolik (1981). Even if in all these objects the $\lambda 1304$ photons are severely affected by the destruction mechanisms described above, they are not sufficient to explain the break of the one-to-one photon relation between $\lambda 8446$ and $\lambda 1304$. TON S 180 is particularly interesting in this respect. We had already seen that it was the only galaxy where the $\mathrm{ROI_{ir}}$ ratio pointed to Lyβ fluorescence as the dominant mechanism for producing $\lambda 8446$. The $\mathrm{ROI_{uv}}$ ratio not only confirms this result but also indicates that the physical conditions of the O I gas is different for this object. Apparently, the optical depth effects that may affect the O I lines do not apply here.

The departure from the one-to-one photon relation can be interpreted as due only to reddening or the combined effects of reddening and the destruction mechanisms of $\lambda 1304$. Columns 2 and 3 of Table 7 list the E(B-V) inferred from the observed flux ratio. Values listed in columns 2 and 3 assume an intrinsic $\mathrm{ROI_{uv}}$ photon ratio of 1 and 1.6, respectively (which translates into a flux ratio of 6.5 and 4). The Galactic extinction curve of Cardelli, Clayton & Mathis (1989) were employed in this calculation.

The E(B-V) derived from the $\lambda 1304/\lambda 8446$ ratio points toward low values of reddening in the BLR of Seyfert 1 galaxies, except in Ark 564, which seems to be affected by a moderate amount of extinction. TON S 180, on the other hand, shows evidence of being reddenning free.

In order to compare the E(B-V) derived from the O I lines with that predicted from other indicators, we have also calculated the reddening using the Balmer decrement Hα/Hβ and the He II $\lambda 1640/\lambda 4686$ ratio. The results are shown in columns 4 and 5 of Table 7, respectively. A "N.A." entry means that that particular ratio was not available for measurement in the spectrum and the lack of any value means that the calculated ratio gave unphysically results (the theoretical values adopted were 3.1 for the Balmer lines and 7.2 for the He II lines). Although the results of Table 7 are approximate, mainly because of the uncertainy involved in the knowledge of the intrinsic ratio of the Balmer decrement and the He II lines for the BLR, it is encouraging to see that the agreement between the different reddening indicators for the same object, are good to within 0.1 mag of uncertainty. In particular, for TON S 180, and Mrk 1044, the three indicators agree to very little or no reddening at all, while for Ark 564, they clearly confirm the presence of dust. The highest discrepancy is observed in 1H 1934-063. This result can be explained if we

consider that the S/N of the UV spectrum is very low and just upper limits to the flux of the lines were derived.

It is also interesting to see that the values of E(B-V) derived assuming an intrinsic $\lambda 1304/\lambda 8446$ flux ratio of 4 are closer to the ones derives using other indicators than if we assume an intrinsic ratio of 6.5 (except for TON S 180). This provides strong observational support to the hypothesis of $\lambda 1304$ photons being destroyed by Balmer continuum absorption and the formation of $\lambda 8446$ by collisional excitation. Although detailed modelling of the BLR is beyond the scope of this paper, it would be important to estimate how much the intrinsic $\lambda 11287/\lambda 8446$ ratio is affected by this latter effect. The data provided here is a good starting point to investigate the physics of the outer BLR.

5.   Summary and Conclusions

Near-infrared, optical and UV spectroscopy has been used to study the excitation mechanisms leading to the formation of permitted O I lines in Seyfert 1 galaxies. From the observed $\lambda 11287/\lambda 8446$ photon flux ratio, we found that in only one out of seven galaxies, Lβ fluorescence is the single dominant process in the formation of O I $\lambda 8446$. This result clearly contradicts previous assumptions that Lβ fluorescence is the only contributor for the formation of the O I lines in those objects. Continuum fluorescence is discarded as an additional mechanism due to the very low O I $\lambda 8446/\lambda 13165$ flux ratio measurement as well as the absence of other emission lines that should be present in the optical region. Recombination is not negligible, although its effects on the flux of $\lambda 8446$ seems to be no larger than a few percent. Collisional excitation offers a plausible explanation to enhance the strength of the O I $\lambda 8446$ relative to that of $\lambda 11287$, leading to the strong deviation from unity observed in the $\lambda 11287/\lambda 8446$ ratio. This conclusion is drawn from the presence of O I $\lambda 7774$ in 1H 1934-063. The strength of this line, relative to that of $\lambda 8446$, agrees with theoretical predictions assuming collisional excitation as responsible for the formation of $\lambda 7774$. In that object, up to 35% of the observed $\lambda 8446$ flux may arise through collisional pumping. Collisional excitation is also favoured if $\lambda 1304$ is optically thick, as is suggested by the presence of strong Ca II lines, which requires high column densities for their formation.

In the absence of reddening, the $\lambda 1304/\lambda 8446$ photon flux ratio may depart from its intrinsic value (from 1 to 1.6) because of several mechanisms that destroy the $\lambda 1304$ photons, as well as optical depth effects that favor collisional excitation of $\lambda 8446$. The agreement between the E(B-V) of the BLR derived using different reddening indicators (among them, the ratio $\lambda 1304/\lambda 8446$) is improved if an intrinsic flux ratio $\lambda 1304/\lambda 8446$ of 4 is assumed, meaning that destruction effects for the $\lambda 1304$ line are, in fact, present. Our results points towards low to moderate reddening for the BLR.

REFERENCES

Boroson, T. A., & Green, R. F. 1992, ApJS, 80, 109

Cardelli, J. A., Clayton, G. C., & Mathis, J. S. 1989, ApJ, 345, 245

Collier, S., Crenshaw, D. M., Peterson, B. M., Brandt, W. N., Clavel, J., et al. 2001, ApJ, 561, 146

Comastri, A., Stirpe, G. M., Vignali, C., et al. 2001, A&A, 365, 400

Ferland, G. J., & Persson, S. E. 1989, ApJ, 347, 656

Giannuzzo, M. E., & Stirpe, G. M. 1996, A&A, 314, 419

Grandi, S. A. 1975, ApJ, 196, 465

Grandi, S. A. 1976, ApJ, 206, 658

Grandi, S. A. 1980, ApJ, 238, 10

Grandi, S. A. 1983, ApJ, 268, 591

Kassebaum, T. M., Peterson, B. M., Wanders, I., Pogge, R. W., Bertram, R., & Wagner, R. M. 1997, ApJ, 475, 106

Kingdon, J., & Ferland, G. J. 1991, PASP, 103, 752

Kwan, J., & Krolik, J. 1981, ApJ, 250, 478

Laor, A., Jannuzi, B. T., Green, R. F., & Boronson, T. A. 1997, ApJ, 489, 656

Morgan, L. A. 1971, MNRAS, 153, 392

Morris, S. L., & Ward, M. J. 1989, ApJ, 340, 713

Oke, J. B., & Shields, G. A. 1976, ApJ, 207, 713

Peterson, B. M., McHardy, I. M., Wilkes, B. J., et al. 2000, ApJ, 542, 161

Persson, S. E., & McGregor, P. J. 1985, ApJ, 290, 125

Rayner, J. T., Toomey, D. W., Onaka, P. M., et al. 2001, PASP, In prep.

Rodríguez-Ardila, A., Viegas, S., Pastoriza, M. G., & Prato, L. 2002, ApJ, Accepted. (astro-ph/0109516).

Rudy, R. J., Rossano, G. S., & Puetter, R. C. 1989, ApJ, 342, 235

Rudy, R. J., Erwin, P., Rossano, G. S., & Puetter, R. C. 1991, ApJ, 383, 344

Rudy, R. J., Mazuk, S., Puetter, R. C., & Hamann, F. 2000, ApJ, 539, 166

Shemmer, O., Romano, P., Bertram, R., Brinkmann, W., Collier, S., et al. 2001, ApJ, 561, 162

Schlegel, D. J., Finkbeiner, D. P., & Davis, M. 1998, ApJ, 500, 525

Stone, R. P. S., & Baldwin, J. A. 1983, MNRAS, 204, 347

Winkler, H. 1992, MNRAS, 257, 677

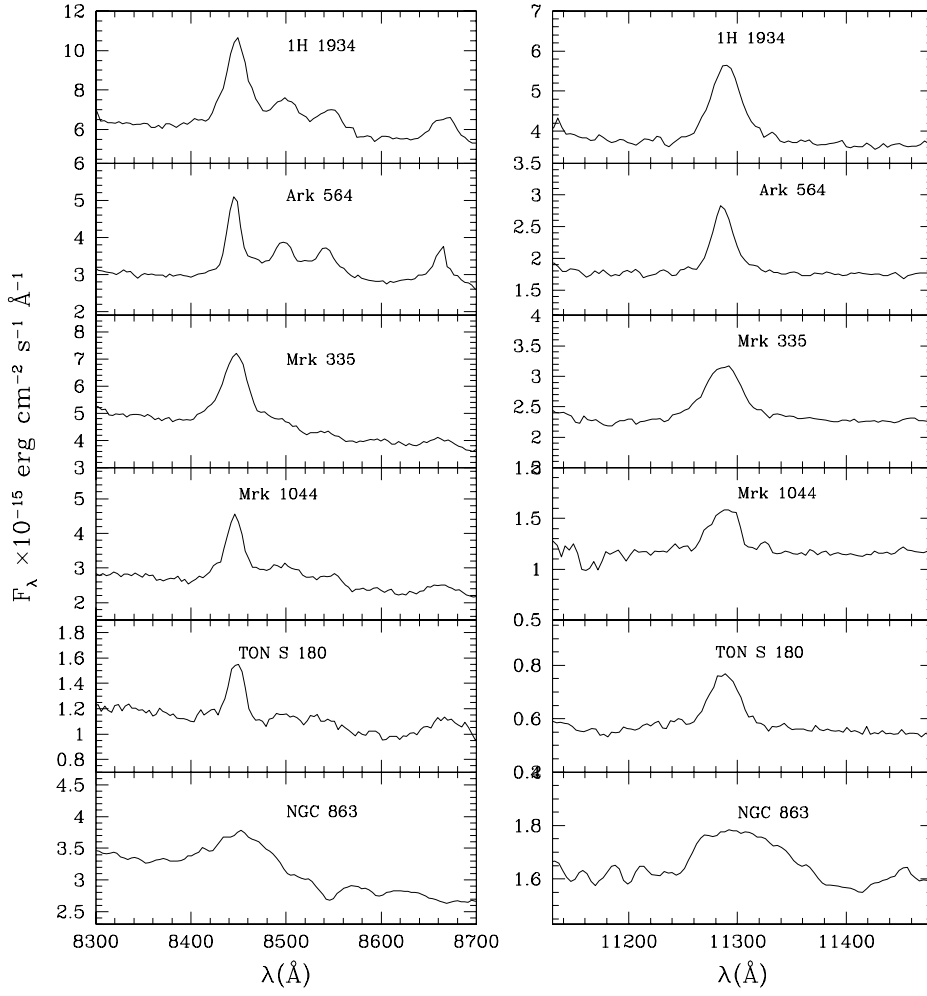Fig. 1.— Observed O I λ8446 (left) and O I λ11287 (right) lines in rest wavelength scale.
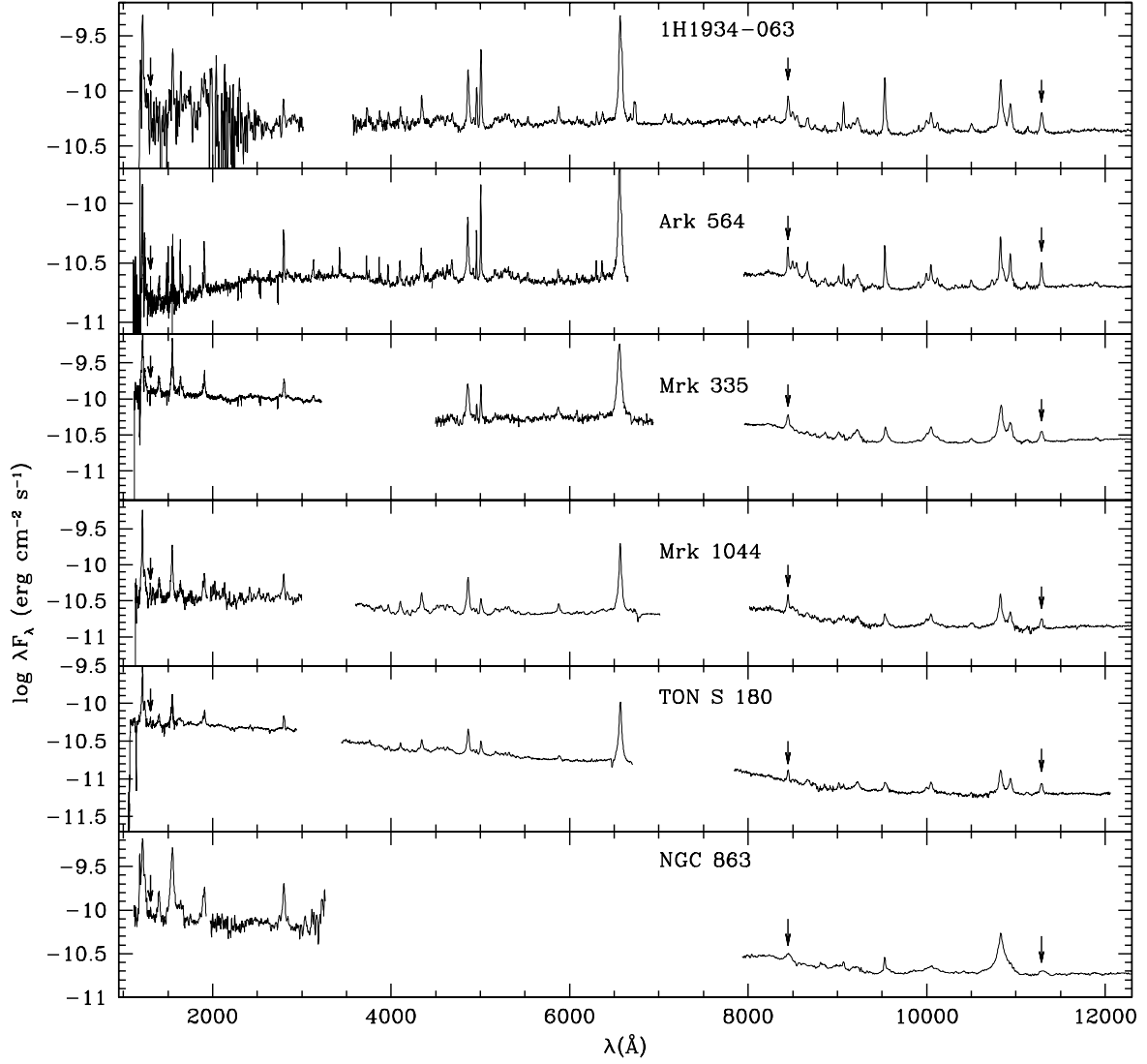
– 16 –

Fig. 2.— Composite UV, optical and near-IR spectra of the galaxy sample. The arrows mark the position of the O I lines at $\lambda1304$, $\lambda8446$ and $\lambda11287$.
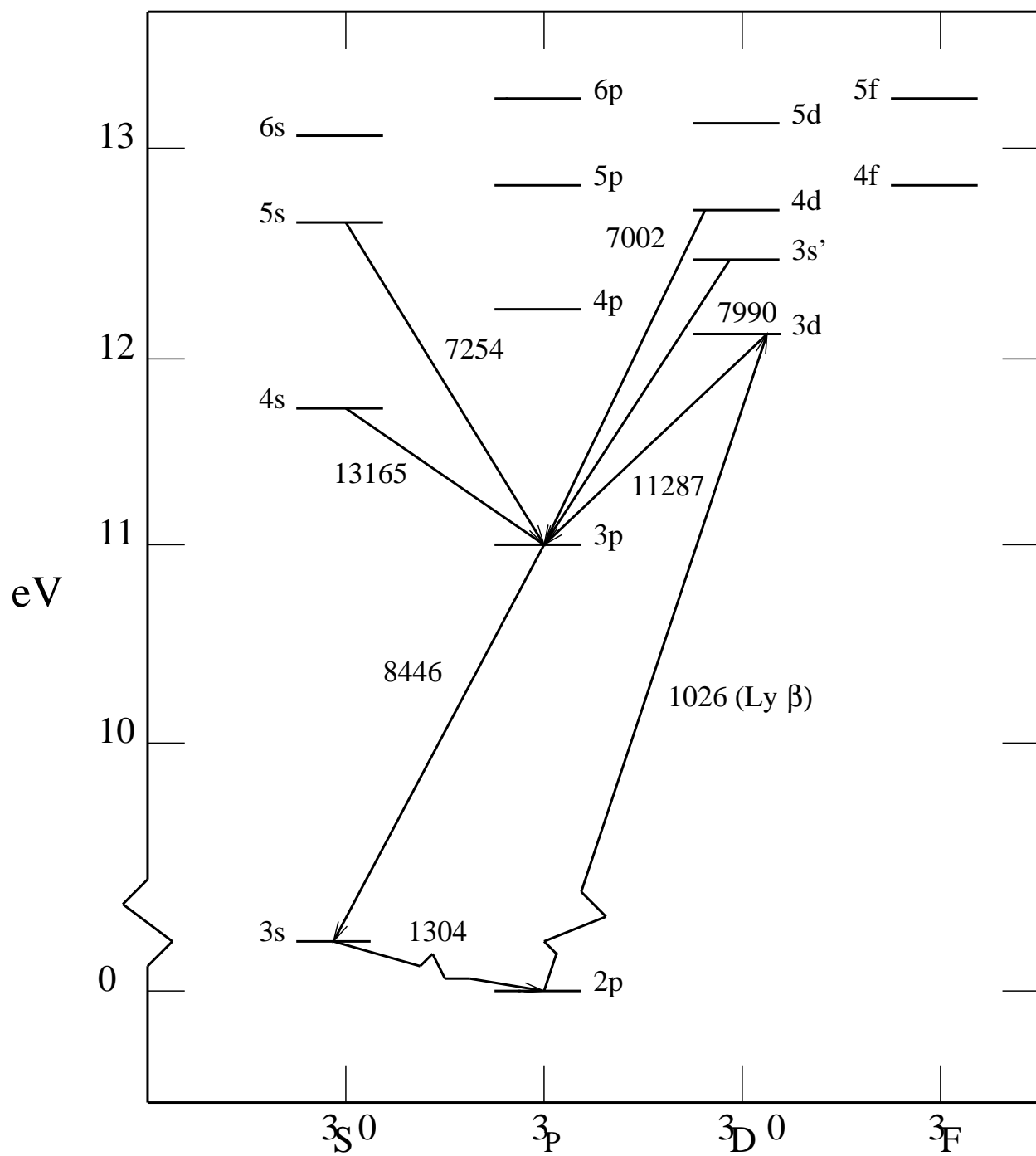
Fig. 3.— Partial Grotrian diagram for the triplet levels of O I, showing the transitions excited by Lyβ.
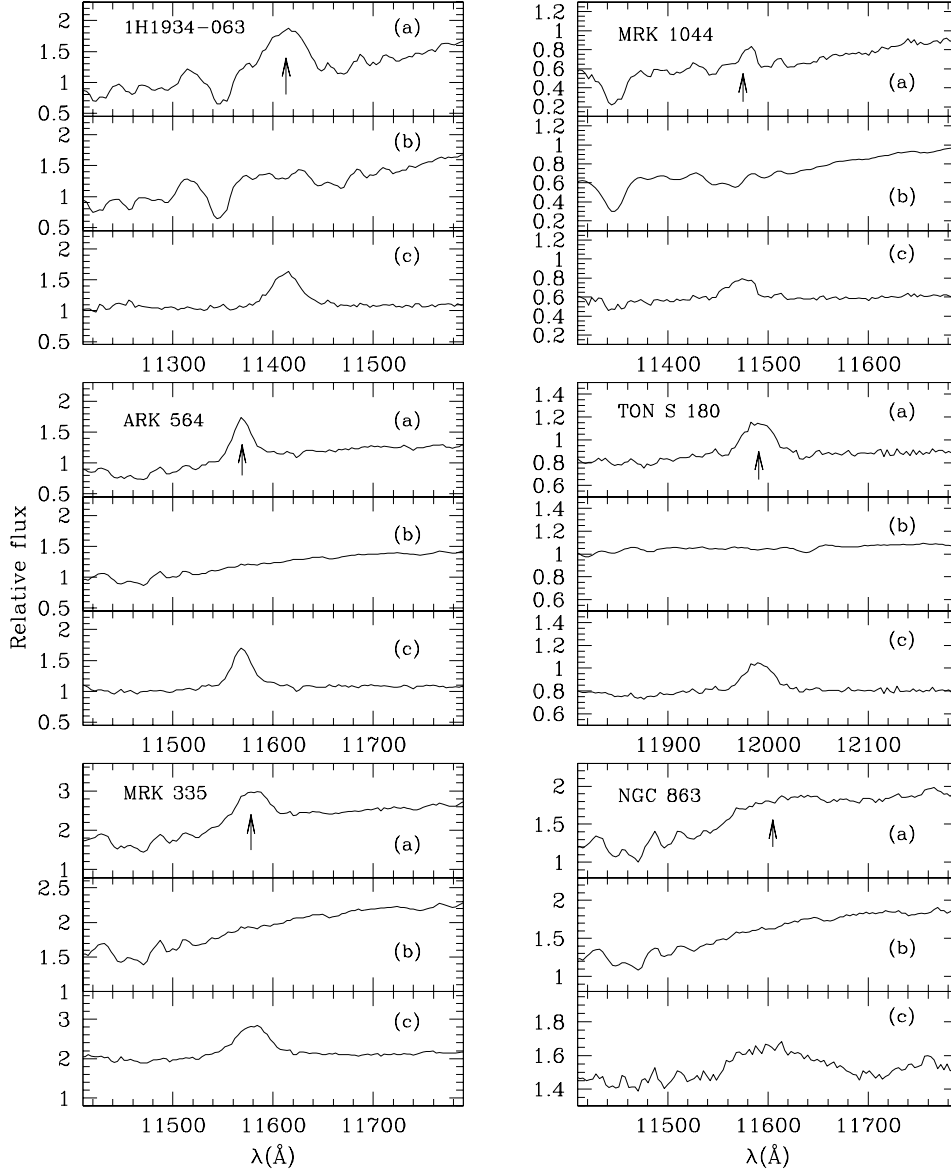
Fig. 4.— Effect of the atmospheric absoprtion on O I λ11287. For each galaxy, panel (a) shows the observed spectrum in the region around that line, in Earth-frame wavelength coordinates. The arrow marks the centroid of λ11287. In (b) it is plotted a sample of the atmospheric transmission in the same spectral region of (a), obtained from the spectrum of a telluric standard near the object's position and observed at a similar airmass. Panel (c) shows the spectrum of the object divided by that of the star. Note that most conspicous atmospheric features dissapeared.
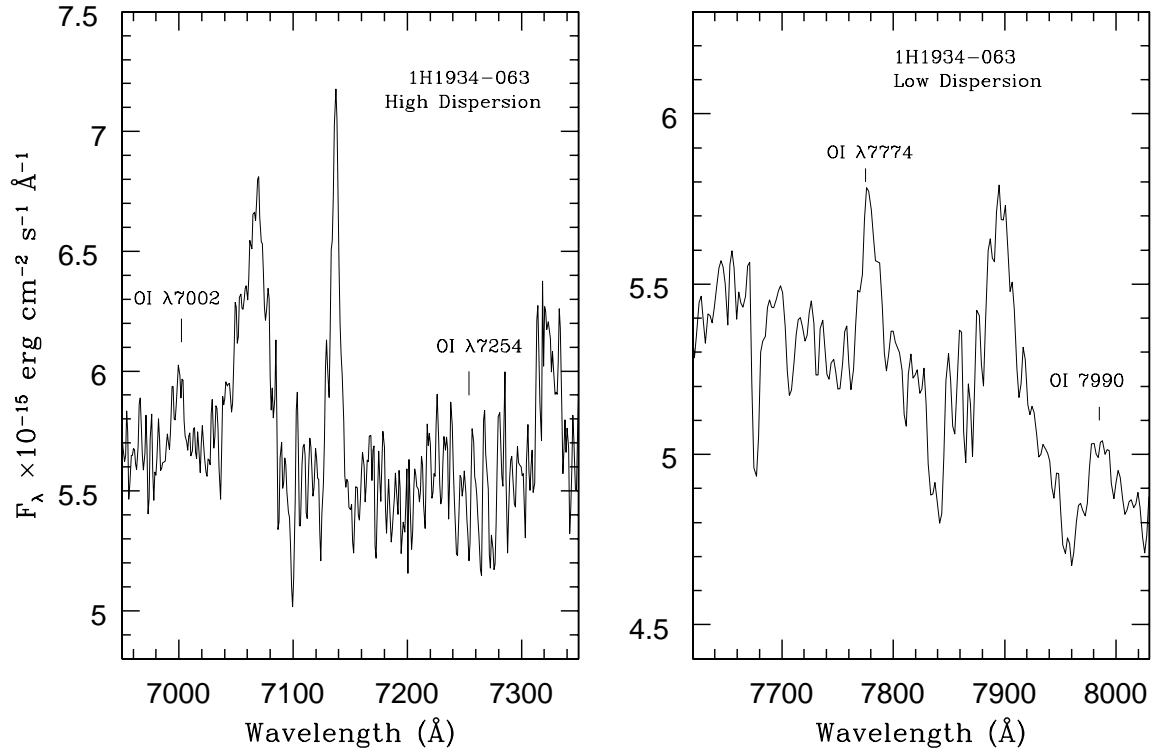
Fig. 5.— Other O I features detected in 1H 1934-063 that arise from processes different to Lyβ fluorescence

Table 1.   Sample characteristics.

Galaxy	z	$M_v{}^a$	$A_v{}^b$	Type
1H 1934-063	0.01059	-19.04	0.972	NLS1
Ark 564	0.02468	-20.42	0.198	NLS1
Mrk 335	0.02578	-21.32	0.118	NLS1
I Zw 1	0.06114	-22.58	0.214	NLS1
Mrk 1044	0.01645	-18.84	0.113	NLS1
TON S 180	0.06198	-22.57	0.047	NLS1
NGC 863	0.02638	-21.27	0.124	Seyfert 1

[a]A value of $H_o = 75$ km s^{-1} Mpc^{-1} was assumed.

[b]Galactic extinction (Schlegel, Finkbeiner & Davis 1998)

Table 2.   Log. of near-IR and optical observations.

Galaxy	Instr./Obs	grating (l/mm)	Coverage (Å)	Exp. Time (sec)	Date of Obs.
1 H1934-063	IRTF	$\cdots$	8000 − 24000	2700	2000 Oct 11
	CASLEO/REOSC	600	6050 − 7600	3600	1996 Aug 10
	CASLEO/REOSC	300	3700 − 6800	3600	1997 Aug 29
	CASLEO/REOSC	300	6500 − 9600	3600	1997 Aug 30
Ark 564	IRTF	$\cdots$	8000 − 24000	2400	2000 Oct 11
	FOS(Y3790406T)	$\cdots$	4500 − 6650	4600	1996 May 23
Mrk 335	IRTF	$\cdots$	8000 − 24000	1800	2000 Oct 11
	CASLEO/REOSC	300	3700 − 6800	1200	2000 Dec 28
Mrk 1044	IRTF	$\cdots$	8000 − 24000	1800	2000 Oct 11
	CASLEO/REOSC	300	3700 − 6800	1200	2000 Dec 28
TON S 180	IRTF	$\cdots$	8000 − 24000	2400	2000 Oct 11
	CASLEO/REOSC	300	3700 − 6800	1200	2000 Dec 29
NGC 863	IRTF	$\cdots$	8000 − 24000	1800	2000 Oct 11

Table 3.   Log. of UV observations.

Galaxy	Inst.	Data Set	Exposure (sec)	Coverage (Å)	Date (UT)
1 H1934-063	IUE/SWP	SWP31894	8400.00	1200 − 2000	1987 Sep 21
Ark 564	STIS	O5IT01010	1201.00	1150 − 1714	2000 May 10
	STIS	O5IT02010	1021.00	1150 − 1714	2000 May 14
	STIS	O5IT03010	1021.00	1150 − 1714	2000 May 19
	STIS	O5IT04010	1021.00	1150 − 1714	2000 May 24
	STIS	O5IT44010	1201.00	1150 − 1714	2000 Jul 6
	STIS	O5IT45010	1201.00	1150 − 1714	2000 Jul 8
	STIS	O5IT46010	1021.00	1150 − 1714	2000 Jul 10
Mrk 335	FOS	Y29E0202T	1390.00	1150 − 1600	1994 Dec 16
Mrk 1044	IUE/SWP	SWP56260	34080.00	1200 − 2000	1995 Dec 7
	IUE/SWP	SWP56319	13499.00	1200 − 2000	1995 Dec 20
TON S 180	STIS	O58P01010	1260.00	1150 − 1714	2000 Jan 22
NGC 863	IUE/SWP	SWP40591	9000.00	1200 − 2000	1991 Jan 14

Table 4.   Fluxes of relevant emission lines.[a]

Line	1H 1934-063	Ark 564	Mrk 335	Mrk 1044	TON S 180	NGC 863	I Zw 1[*]
O I λ1304	<18.0[b]	2.00±0.20	10.9±1.0	13.6±2.00	5.74±0.7	6.70±1.0	<10.0
He II λ1640	<56.5	11.8±0.70	63.0±5.0	24.2±3.6	7.15±1.50	25.7±4.0	$\cdots$
He II λ4686	7.00±0.80	3.80±0.20	31.0±3.0	4.48±0.5	1.21±0.15	$\cdots$	$\cdots$
Hβ	41.83±3.0	22.8±0.8	76.5±7.0	26.8±2.0	14.5±1.0	$\cdots$	$\cdots$
Hα	129.7±5.0	92.3±1.0	320±10	67.4±4.0	43.0±2.0	$\cdots$	$\cdots$
O I λ8446	14.5±1.0	4.40±0.10	8.14±0.5	4.96±0.4	0.98±0.10	4.01±0.30	8.83±1.0
O I λ11287	6.91±0.24	2.70±0.07	3.87±0.17	1.52±0.17	0.80±0.09	1.65±0.2	5.00±0.4
O I λ13165[c]	<0.17	<0.18	<0.20	<0.22	$\cdots$	$\cdots$	$\cdots$

[a]In units of 10^{-14} erg cm^{-2} s^{-1}.

[b]The < sign implies an upper limit.

[c]In TON S 180 and NGC 863 O I λ13165 falls within an atmospheric absorption band, so it is not possible to derive an upper limit.

[*]Fluxes taken from Rudy et al. (2000)

Table 5. Measured $\mathrm{ROI_{IR}}$ and $\mathrm{ROI_{uv}}$ flux and photon ratio for the galaxy sample.

Galaxy	$\mathrm{ROI_{IR}}$		$\mathrm{ROI_{uv}}$	
	Flux	Photon	Flux	Photon
1H 1934-063	0.48±0.04	0.64±0.05	1.25[a]	0.19[a]
Ark 564	0.61±0.02	0.82±0.03	0.45±0.05	0.07±0.01
Mrk 335	0.48±0.04	0.64±0.05	1.33±0.15	0.20±0.02
Mrk 1044	0.31±0.04	0.42±0.05	2.78±0.47	0.43±0.07
TON S 180	0.81±0.12	1.08±0.16	5.88±0.98	0.91±0.15
NGC 863	0.41±0.06	0.55±0.08	1.70±0.28	0.26±0.04
I Zw 1	0.56±0.08	0.76±0.11	1.14[a]	0.18[a]

[a]Upper limit

Table 6.   Fluxes measured to other O I features[a]

Line	1H 1934-063	Ark 564	Mrk 335	Mrk 1044	TON S 180
$\lambda6046$	<4.6	<1.5	<2.3	<2.4	<0.9
$\lambda6726$	<6.0	...	<2.1	<1.3	...
$\lambda7002$	4.0±0.8	...	...	...	...
$\lambda7254$	<3.9	...	...	...	...
$\lambda7774$	10.0±0.8	...	...	...	<0.8
$\lambda7990$	5.1±0.9	...	...	...	<0.9
$\lambda8446$	145.0±10	44.0±1.0	81.4±5.0	49.6±5.0	9.8±1.0

[a]In units of 10^{-15} erg cm^{-2} s^{-1}. Lines with the < sign indicate an upper limit.

Table 7.   Derived E(B-V) from the O I lines and other reddening indicators.[a]

Galaxy	R OI$_{uv}$		Hα/Hβ	He IIλ1640/λ4686
	(6.4)	(4.0)	(3.1)	(7.2)
1H 1934-063	0.23	0.15	0.0	...
Ark 564	0.36	0.29	0.26	0.22
Mrk 335	0.21	0.15	0.30	0.34
Mrk 1044	0.11	0.05	0.0	0.06
TON S 180	0.01	0.00	0.0	0.05
NGC 863	0.18	0.11	N.A.	N.A.
I Zw 1	0.24	0.17	N.A.	N.A.

[a]The value in parenthesis below the reddening indicator corresponds to the intrinsic ratio assumed